

# Accelerator Mass Spectrometry: Ultra-sensitive Detection Technique of Long-lived Radionuclides

Hans-Arno Synal\*

**Abstract:** An introduction is given to accelerator mass spectrometry (AMS) technology, to the fundamental measurement principles, and the physics aspects behind the design constraints of AMS instruments. This article shall give an overview on technical design constraints of AMS instrumentation, general ion optical principles, and nuclide specific problems. The historic development of AMS detection techniques is briefly summarized. The wide variety of applications connected to the AMS technology are not discussed.

**Keywords:** AMS · Charge exchange · Long-lived radionuclide detection · Molecule dissociation



**Hans-Arno Synal**, accelerator mass spectrometry specialist with a background in nuclear and atomic physics, studied Physics at Rheinische Friedrich-Wilhelms-Universität Bonn, and graduated in 1985. He moved to Swiss Federal Institute of Technology Zurich (ETHZ) and obtained his PhD on ‘Accelerator mass spectrometry with  $^{36}\text{Cl}$ ’ in 1989. Following a post-doctoral fellowship at the Institute of Intermediate Energy, ETH Zurich, he became research scientist at the Paul Scherrer Institute. Since 2008, he is heading the ETH Laboratory of Ion Beam Physics (LIP) and he was appointed as honorary Professor at ETH Zurich in 2011.

## 1. Introduction

Radioactivity is often perceived as a threat because of the enormous energy release during a single nuclear transformation. But it is precisely this fundamental property that ultimately causes it to disappear and according to the half-life of the nuclides, their number decreases exponentially. Thus, only a few surviving radionuclides exist on Earth today, which were created during the stellar explosion of the precursor star of our solar system. In general, detection of radionuclides is relatively easy since radioactive decay is accompanied by high-energy radiation and a single decaying atom can be detected. For long-lived nuclides, however, the decay probability is so low that many nuclides must be present to detect a statistically significant number of decays within a reasonable time. Not only primordial radionuclides are found in nature today. Radionuclides are constantly being produced in connection with the decaying primordial radionuclides U and Th as well as from the radiation generated by their decay products. In addition, they are produced by cosmic radiation, and artificially produced nuclides from the worldwide military and civil nuclear activities are found in the environment. Their well-defined source mechanism is a great advantage. It enables us to use them as tracer substances. Natural production rates are usually very low, and these nuclides occur in extremely low isotope ratios compared to their stable isotopes. Typically, they are within a range of  $10^{-9}$  to

$10^{-15}$  or even below. This makes detection using conventional mass spectrometers practically impossible.

In the middle of the last century, when the properties of  $^{14}\text{C}$  were studied, attention was also focused on its decay properties when it was discovered that the activity of dead organic material was an exceptional measure for dating its origin.<sup>[1]</sup> It was clear early on that with a half-life of 5700 years, direct mass spectrometric detection of individual atoms is many times more efficient than patiently waiting for individual decay events.<sup>[2]</sup> But the almost infinite surplus of stable carbon isotopes and the presence of practically equal-mass nuclear and molecular isobars put paid to the dream of directly counting the  $^{14}\text{C}$  atoms. Only when it was realized that the nuclear  $^{14}\text{C}$  isobar  $^{14}\text{N}$  could be completely suppressed by creating negatively charged ions<sup>[3]</sup> and with the knowledge that interfering mass-equivalent molecules can be completely broken up into atomic ions by the charge changing process in the stripper of a tandem accelerator<sup>[4]</sup> the possibility for mass spectrometric  $^{14}\text{C}$  detection appeared.<sup>[5]</sup> This discovery was the birth of accelerator mass spectrometry (AMS), which spread rapidly as the huge potential and enormous advantages of using direct  $^{14}\text{C}$  detection were immediately recognized. Today, there is a wide variety of radionuclides which are routinely analysed with AMS systems.<sup>[6]</sup> Radiocarbon is still the most important and, based on its unique biochemical behavior, has countless applications.  $^{10}\text{Be}$ ,  $^{26}\text{Al}$ ,  $^{36}\text{Cl}$ ,  $^{41}\text{Ca}$ ,  $^{129}\text{I}$ ,  $^{236}\text{U}$ , and nuclides of the actinide series can be regarded as standard AMS nuclides with versatile applications in earth/environmental sciences as well in bio-medical application, nuclear forensic, and many other research fields. In addition, there are more exotic nuclides such as  $^{32}\text{Si}$ ,  $^{53}\text{Mn}$ ,  $^{60}\text{Fe}$ ,  $^{63}\text{Ni}$  and others that have been measured using AMS technology in various applications. The focus of this article is the basic technology which makes the detection of such nuclides at their natural abundance level possible.

## 2. Characteristics of AMS Systems

A typical AMS setup as shown in Fig. 1 has the following main components: i) ion source, ii) pre-acceleration mass filtering system, iii) acceleration stage with charge exchange and molecule dissociation unit, iv) post acceleration mass filtering

\*Correspondence: Prof. H.-A. Synal, E-mail: synal@phys.ethz.ch, Laboratory of Ion Beam Physics, ETH Zurich, CH-8093 Zurich

stage, and v) particle identification and beam quantification devices. This general layout may have a large variety of possible configurations, but you will find the basic design elements in any AMS system. In general, there are four important considerations that need to be addressed to reach the required sensitivity:

- suppression of isobaric interferences,
- sufficient abundance sensitivity,
- reliable normalization procedure,
- unambiguous identification of ions.

Not all these requirements can be met at once and separate filter stages, each optimized for a specific separation mechanism, are typically connected in a chain. This principle can be regarded as the key to direct detection of radionuclides at their natural abundance levels.

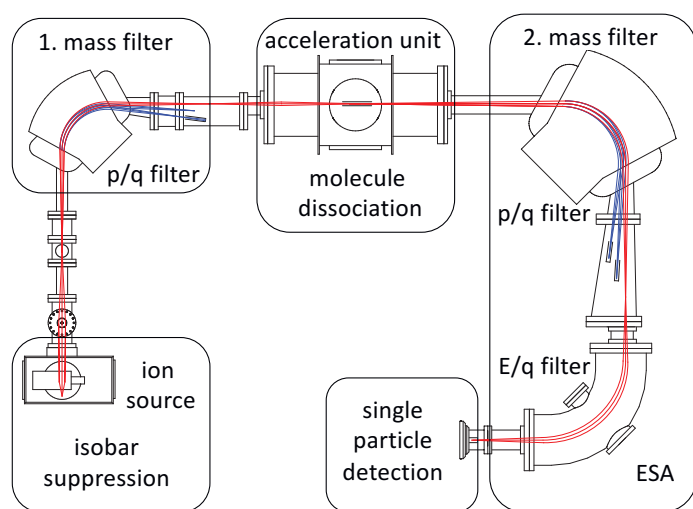


Fig. 1. Schematic layout of an AMS system based on the MICADAS system design.

## 2.1 Equal Mass Interferences

We distinguish between nuclear and molecular species, which must be eliminated as far as possible. Mass differences of nuclear isobars are extremely low as can be seen for the isobar pair  $^{14}\text{C}/^{14}\text{N}$  where the relative mass difference is about  $10^{-5}$ . Modern high-resolution mass spectrometers will be able to resolve such tiny mass differences but only if the two species will have comparable intensities. This is not the case for practically all AMS radionuclides. The problem can be avoided in cases where the interfering nuclear isobar does not form stable negative ions. This is possible for  $^{14}\text{N}/^{14}\text{C}$  and  $^{26}\text{Mg}/^{26}\text{Al}$ , but also noble gas isobaric interferences such as  $^{36}\text{Ar}/^{36}\text{Cl}$  or  $^{129}\text{Xe}/^{129}\text{I}$  can be eliminated in the same way. Specific molecules can be used for which the interfering nuclear isobar will not form stable negative ions. Typical examples are:  $^{41}\text{KH}_3/^{41}\text{CaH}_3$  and  $^{41}\text{KF}_3/^{41}\text{CaF}_3$  which yield a substantial suppression of  $^{41}\text{K}$  and  $^{60}\text{FeH}$  where  $^{60}\text{NiH}$  can be reduced. If isobaric interference cannot be eliminated or significantly reduced already with the negative ion formation process, techniques of ion interaction with matter are applied. Here, a high ion energy is advantageous and AMS systems based on large accelerators (6–15 MV terminal voltage) can reach good isobar suppression for medium heavy nuclide up to iron making use of energy loss characteristics. Ion interaction with Laser light,<sup>[7]</sup> by exploiting molecular instabilities, or charge exchange reactions in buffer gases<sup>[8]</sup> are attractive alternatives. This opens new opportunities because suppression of isobars can be achieved already at the low energy end of the AMS system, and several new radionuclides come into the reach of the AMS technology.<sup>[9]</sup>

An elegant way to separate molecules of the equal mass results from the charge changing process in the terminal of a tandem ac-

celerator. The negative ions, which are accelerated to high energies, lose all or part of their bonding electrons through collisions with neutral atoms or molecules. They will generate a charge state distribution after passing through a stripping medium where the mean charge state depends on the speed of the colliding ions. Decisive for yield of individual charge states are the cross-sections for the electron capture and loss reactions in the respective collision processes. Molecules become unstable as soon as sufficient bonding electrons are removed. Only atomic ions remain after molecules have passed a stripping medium at sufficient velocity to populate  $3^+$  and higher charge states. The instability of light molecules against Coulomb force and the need to exploit highly charged ions ( $>3^+$ ) has been a ‘golden rule’ for many years for the design of AMS systems. The beauty of getting rid of interfering molecular interference comes at the price of high ion energies. For radiocarbon, approximately 2.5 MeV ion energy is needed to reach the maximum stripping yield of  $3^+$  ions (33%) with Ar.<sup>[10]</sup> In case of  $4^+$  the yield is significantly higher (65%) but can only be reached at 6.5 MeV. This is the reason why conventional AMS systems cannot be regarded as ‘mass spectrometers’ in a true sense. They are much more complex accelerator infrastructures as they were common in traditional nuclear physics research institutions. By realizing that the molecular ions can be dissociated in collisional reactions if the  $1^+$  charge state is used,<sup>[11]</sup> a groundbreaking step forward to build compact AMS systems was reached.

## 2.2 Abundance Sensitivity

Natural isotopic ratios of long-lived radionuclides relative to their most abundant stable isotope are well below the abundance we can find of almost any element in common materials. To reach such a sensitivity, the approach applied to suppress molecular interferences is helpful. It requires a multi-stage mass analyzing set-up. In a first step, ions are selected for the mass of the radionuclide of interest. Magnetic sector fields are used for light ion species and combinations of magnetic and electrostatic sector fields (ESA) are common for the analysis of ions at the upper end of the periodic table. Such a preselected ion beam consists primarily of molecular species. They are broken-up during the stripping process and a second stage mass filtering system will separate the molecular breakup products from the radionuclides which are all atomic ions. This is easy because of the substantial mass differences between neighboring isotopes. However, a true mass selecting system combining momentum over charge (p/q) and energy over charge (E/q) filtering is needed to unambiguously separate the radionuclide ions. In practice, this is more challenging since the molecular break-up products occur in various charge states, may undergo collisional processes with residual gas, apertures, or parts of the beam line system, and finally may end as interfering background in final detection. A careful design of the second stage spectrometer is essential and parasitic beam components that potentially could be the cause for misidentified ions need to be identified to minimize instrumental backgrounds.

## 2.3 Normalization Procedure

An AMS system measures isotope ratios. Both the individually identified radionuclide ions and the intense currents of the associated stable isotopes must be analyzed. For radiocarbon detection these are typically  $\approx 200$  cps, and  $\approx 100 \mu\text{A}$  ( $^{12}\text{C}^-$ ), respectively. This should be done under conditions that are as comparable as possible. AMS systems are usually equipped with fast beam switching systems.<sup>[12]</sup> The stable and the rare isotope beams can be alternately injected into the accelerator stage in short pulses and the different isotopic beams are separated again after the first mass dispersive element following the acceleration stage. Faraday cups are used to measure the electrical current of the stable isotope beams, whereas the rare isotope will further

pass filtering elements, *e.g.* an electrostatic analyzer to get rid of interfering particles that still may be part of the ion beam. The similar beam transport conditions for radionuclide and stable isotopes result in reproducible isotopic ratio measurements. For radiocarbon, two stable isotopes are measured. This offers the possibility to trace isotope fractionation that occur not only during beam transport but also during sputtering and the sample preparation process. By applying a fraction correction based on the measured  $\delta^{13}\text{C}$  of the individual samples, the most reliable  $^{14}\text{C}/^{12}\text{C}$  ratios can be determined. Standard reference materials are used to obtain adequate correction factors to finally determine absolute isotope ratios.

### 2.4 Detection of Individual Ions

Gas ionization chambers are the detection systems of choice. At high ion energies, energy loss of swift ions in a detector gas can be used to separate isobaric ion pairs. At the very end of an AMS system, ions will have the same energy before they enter the detection system. Since stopping power of swift ions is related to their nuclear charge, the energy release during stopping process provides a characteristic charge signal along the stopping path. By collecting this charge cloud in several detector sections, identification of ion species can be made (Fig. 2). Unambiguous detection is given, and dark pulses are negligible if there are no particles reaching the detector. Developments of gas ionization detectors for isobar separation originate from early nuclear physics experiments<sup>[13]</sup> and the technology has been adopted to the needs of AMS detection.<sup>[14]</sup> Silicon nitrate membranes have been introduced as gas ionization detector windows and a significant improvement in the detection of low energetic ions has been achieved.<sup>[15]</sup> Reducing parasitic capacitances and improving detector readout electronics<sup>[16]</sup> have made these detectors robust and reliable to operate. Special designs even allow detection of carbon ions at ion energies of less than 50 keV.<sup>[17]</sup>

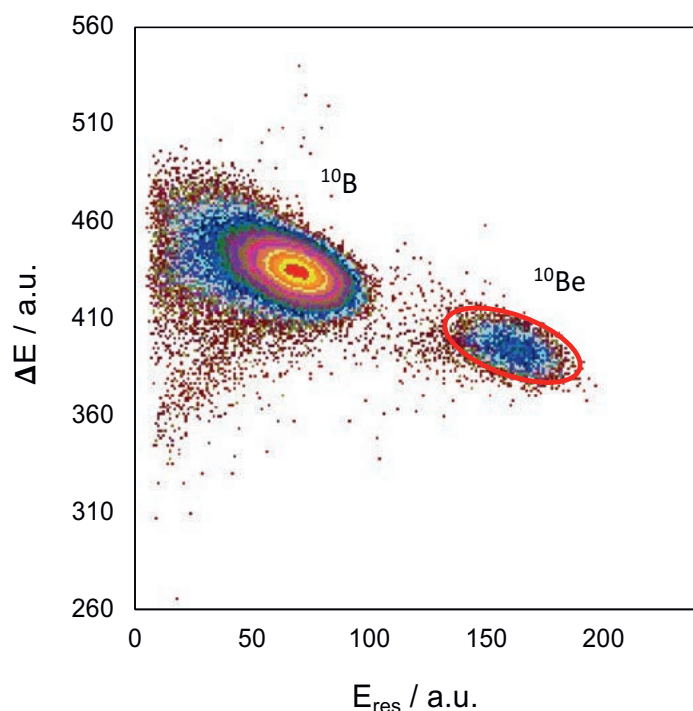


Fig. 2. Particle identification of  $^{10}\text{Be}$  using energy loss characteristics.  $\Delta E$  denotes the energy loss in the first part of the detector,  $E_{\text{res}}$  the residual energy. A clear separation of  $^{10}\text{Be}/^{10}\text{B}$  is visible.

### 3. Ion Optical Considerations

Crucial for the precision of AMS measurements is a high ion-optical transmission of the spectrometer. Ion generation during sputtering is defining the initial space volume which is of the order of  $2\text{--}5 \pi \times \text{mm} \times \text{mrad MeV}^{1/2}$ . Divergence of the ion beam is reduced by acceleration but collisional processes during charge exchange and molecule destruction will increase beam divergence. To minimize this additional component to the phase space volume, a beam waist is formed at the stripper center, and the two mass separators, at low energy end and high energy end, respectively, can be regarded as independent ion optical components. Foil or gas stripping can be used to convert negative ions into a positive charge state. Foil stripping (typically self-supporting C-foils) is preferred if high ion energies are needed. Stripping foils have a typical areal density of a few  $\mu\text{g}$  per square centimeters, they are not very homogeneous, and they degrade from the constant bombardment with the ion beam. All this introduces energy and angular straggling to the ion beam distorting the beam quality and causing beam losses. With gas as stripping medium, the latter two disadvantages of foil stripping can be overcome. But it is difficult to confine the stripper gas into a specific volume and to reach the necessary areal densities in a windowless gas target configuration for equilibrium charge exchange and molecule dissociation conditions. Helium is the best suited stripping medium in AMS system operating in the sub-MeV energy range.  $\text{N}_2$  or Ar as stripper gases can be pumped better and are used at large AMS accelerators where angular straggling during the stripping process is less important.

The electrical field of the acceleration section causes a strong lensing action at the entrance of the accelerator. Phase space of the ion beam extracted from the ion source and acceptance of the accelerator is matched by creating a beam waist situation inside the stripper canal. In traditional AMS setups, a double lens system in a telescope configuration is often used to match waist position for various ion energy and terminal voltage combinations. This requires some distance causing a quite large footprint. AMS systems based on High Voltage Engineering Europe, Netherlands, (HVE) accelerators are equipped with the patented Q-snout<sup>[18]</sup> system which results in a very compact layout of the system. In compact AMS systems from ETHZ, Ionplus AG, Switzerland, and National Electrostatic Corporation, USA, (NEC) the beam waist formed right after the first mass filtering stage is acting as a beam optical object to produce a waist-to-waist image at the stripper center.<sup>[19]</sup> Similar considerations are made to get optimum beam transport from the ion source through the initial mass separator. Typically, the lensing action given by the extraction electrodes is supplemented with a second lens to form a telescope setup. Thus, the ratio of spatial beam size versus the maximum beam divergence can be tuned to match the best suited conditions (Fig. 3). The stripper at the center of the acceleration system can be regarded as a new ion optical object and further beam transport can be calculated independently. The related phase space volume is given by the geometry of the stripper tube itself whereas its internal diameter is defining the spatial waist dimension and the solid angle of the tube gives the maximum beam divergence. Acceleration of the ions emerging from the stripper tube compresses beam divergence. It is related to the energy gain of the ions and thus depending in the individual charge state of ion. A virtual beam object is formed not exactly at the stripper center but displaced towards the low energy end of the acceleration unit. It is acting as a beam object of the further beam transport. The higher the charge state of the ion the higher is the energy gain and the virtual object moves further away from the stripper center. In dedicated radiocarbon AMS systems using  $1^+$  charge the most compact design simply uses this virtual object for the beam transport through a second stage mass spectrometer (Fig. 4a). Instruments designed to measure ions in different charge states incorporate electrostatic lenses to matched

ion optical coupling of virtual beam object points to the follow-up mass filtering spectrometer. This can be achieved either by matching phase space volume directly to the acceptance of the next dispersive beam optic element (Fig. 4b), or by forming again an intermediate waist point behind the accelerator exit (Fig. 4c). Matching the gaps of all beam optic elements to the maximum possible beam divergence enables a lossless beam transport at the high energy end of the AMS system. Today, detailed beam optic calculations based on matrix codes in combination with Monte Carlo simulation tools are applied to push beam optics towards the physical limits.<sup>[20]</sup> In case of dedicated radiocarbon detection systems, this can be as high as 95% in total.

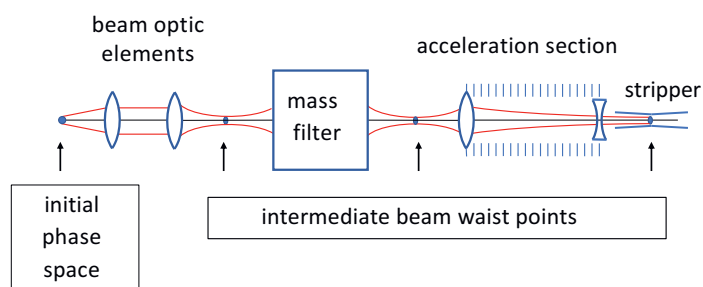


Fig. 3. Beam transport at low energy end of an AMS system.

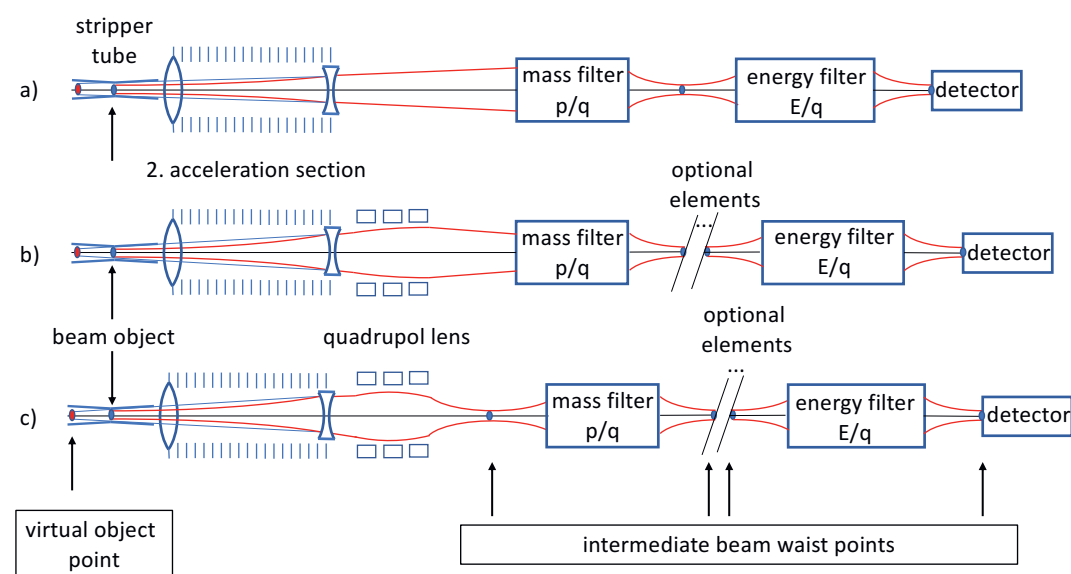


Fig. 4. Schematic ion optics at HE end of AMS systems: a) for ions in one specific charge state, b) adoption of focussing properties for ions in different charge states with quadrupole lens, b) without, and c) with intermediate beam waist.

#### 4. Physics of Low Energy AMS

Reducing ion energy is the key to design AMS instruments that can be regarded as true mass spectrometers. At lower acceleration voltages the yield of carbon ions in charge states  $3^+$  decreases rapidly and efficient  $^{14}\text{C}$  detection becomes impossible. Already in the early 1980s, it had been shown<sup>[21]</sup> that beam intensities of molecular carbon ions in charge states  $1^+$ , and  $2^+$  can be reduced during transition from negative to positive charge states. These experiments had been performed at an AMS instrument that didn't allow to retrieve information on the actual target density present in the stripper canal other than a proxy pressure measurement within the beam transport system. Thus, cross sections for dissociation of mass 14 molecules ( $^{12}\text{CH}_2$ ,  $^{13}\text{CH}$ ) could not be extracted. With

measurements of these cross sections in  $\text{N}_2$  or He gases<sup>[11a,22]</sup> the feasibility of low energy AMS could be explored and design parameters of compact AMS systems could be determined.<sup>[23]</sup> The molecule dissociation cross sections as illustrated in Fig. 5 are of the order of the geometric size of the molecules<sup>[24]</sup> and show only a weak energy dependency for He stripper gas. A sufficient rate of molecule dissociation can be reached with He stripper gas at areal density of  $\approx 0.5 \mu\text{g}/\text{cm}^2$ .<sup>[24]</sup> The second important constrain is the yield of  $1^+$  carbon ions as function of ion energy. Helium gas features a  $1^+$  efficiency of more than 50% and a rather unexpected increase with decreasing ion energy in the range between 50–200 keV. This can be explained by the small electron-capture cross sections due to the strong bonds of He k-shell electrons in this energy range.<sup>[25]</sup> Helium gas has the advantage that scattering cross sections are significantly smaller than for heavier stripper gases leading to lower beam losses. Multiple scattering can be calculated using the Sigmund model<sup>[26]</sup> and design parameters on the geometry layout of stripper canal as well as the acceptance of the beam optics components at the HE end of the AMS system can be determined. They can be improved with Monte Carlo techniques which are following individual ion paths through the gas stripper, simulating collisions, related energy loss and respective change of flight direction.<sup>[20]</sup> But not only for  $^{14}\text{C}$  AMS, He gas stripping is advantageous. For actinide ions, a stripping yield for the  $3^+$  charge state of more than 45% can be reached at 500 keV ion energy.<sup>[27]</sup> Molecules in this mass range can form triply positively charged ions<sup>[28]</sup> and the stripper gas density needs to be set to higher values as they would be needed to reach the charge state equilibrium. Therefore, transmission losses from the increased

angular and energy straggling are encountered. Still, more than 30% overall transmission is possible at optimized low energy systems<sup>[29]</sup> which, compared to setups at large AMS systems is at least a factor of five higher.

#### 5. Constraints for Universal AMS Systems

There is a class of AMS instruments that are designed to measure more than one specific radionuclide. These 'universal' AMS systems require a more advanced ion optical setup. Whereas a combination out of a magnetic and electrostatic sector field is already sufficient to separate the  $^{14}\text{C}$  ions,<sup>[30]</sup> more complex setup is needed for the other AMS nuclides, and the beam line is often extended with an additional filter element to further suppress un-

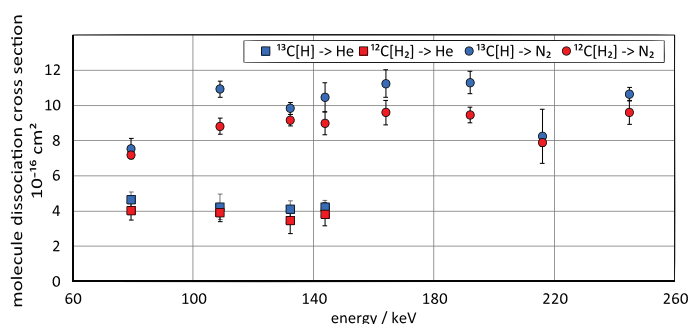


Fig. 5. Molecular dissociation cross sections for light carbon molecules in He and  $\text{N}_2$  gases adopted from Schulze-König.<sup>[24]</sup>

wanted background events at the detector. The mass of the heaviest nuclide to be detected constrains to a large extent the overall dimensions of the AMS instrument. Conventional electromagnets will go not much higher than 1.3 T of magnetic flux density inside a decent gap. Therefore, bending radii of already 0.6 m are required to analyze  $^{236}\text{U}$  ions having charge state  $3^+$  and ion energy of 1.12 MeV. Traditional multi-isotope AMS system with 3 MV accelerators such as the Vienna Environmental Research Accelerator (VERA<sup>[31]</sup>) host even larger magnets (e.g. 1.27 m bending radius). At AMS facilities based on accelerators with 5–14 MV terminal voltage  $\approx 2$  m radii are common.

AMS measurements of nuclides at the upper end of the periodic table will face the problem that mostly no stable isotopic counterpart to the rare isotope is available to obtain isotopic ratios. In such cases, spikes of artificially produced isotopes are used instead. This makes the detection of two or more nuclides with a particle detection system necessary, and the individual isotope ion beams need to follow all filtering elements up to the final particle detector. An elegant way to enable ion transport of different isotopes through  $p/q$  filtering elements is a beam switching system as it is commonly incorporated at injection magnets of AMS systems. But the ions will have energies in the low MeV range and the voltages required to match magnetic rigidities of different isotopes are much higher. For isotopes of actinide series, related energy differences can still be matched by biasing the vacuum chamber of the magnets, with switching power supplies (20 kV).<sup>[32]</sup> A feasible alternative is to adopt ion energy of different isotopes by changing the terminal voltage of the accelerator and settings of the ESA electric field accordingly to let the ions pass and get them to the final detector. A detailed description of such a procedure is given by Christl.<sup>[29]</sup> An AMS system covering the full mass range of the periodic table can easily be tuned to detect other standard radionuclides such as  $^{26}\text{Al}$ ,  $^{41}\text{Ca}$ , and  $^{129}\text{I}$  and there are no further constraints to the ion optics.

## 6. Historic Aspects

For many years the AMS technology had been driven by the needs of the applications. Although there are more than 40 nuclides<sup>[6]</sup> that have been used with AMS instrumentation, radiocarbon is still of paramount importance. Dedicated instruments have become available, starting with the very first commercial AMS systems developed by Kenneth Purser<sup>[12a]</sup> (General Ionex), one of the early pioneers in the AMS history. Based on the idea to dissociate molecular interferences in a Coulomb explosion process, accelerator systems with nominal 3 MV terminal voltage were needed and AMS systems with quite large footprint and the related complex infrastructure had to be maintained. During the early time of AMS, several laboratories explored their potential to detect other nuclides than  $^{14}\text{C}$ . Tandem accelerator facilities originally designed for fundamental nuclear physics research were converted into dedicated AMS systems, requiring an even more demanding infrastructure environment. The first ‘third-generation’  $^{14}\text{C}$  dedicated AMS instrument was designed in

connection with the World Ocean Circulation Experiment (WOCE) to monitor  $^{14}\text{C}$  in the global oceans.<sup>[33]</sup> At the Woods Hole oceanographic institution, such a 3 MV  $^{14}\text{C}$  AMS system was installed in 1990<sup>[34]</sup> and became fully operational in 1993.<sup>[35]</sup> HVE commercially built several similar instruments and in the 1990s they were leading the market of commercial AMS instruments. In 1998, the first system using collisional molecule break-up became operational at ETH Zurich<sup>[11b]</sup> with performance comparable to traditional AMS. This type of instrumentation was commercialized by NEC, and a first system was installed at the University of Georgia<sup>[36]</sup> followed by about 20 similar systems around the world. Based on this technology, NEC developed a single stage AMS system (SSAMS)<sup>[37]</sup> where the stripper unit and the following mass spectrometer is installed at an open stack 250 kV high voltage platform and today, there are 13 SSAMS instruments in operation. HVE realized the advantages of the compact AMS system and developed a multi-nuclide AMS system<sup>[18]</sup> based on a 1 MV Tandatron accelerator. The first instrument was installed at University of Seville in 2005.<sup>[27]</sup> In total more than 10 instruments of this type are in operation.

The next step to further reduce complexity of dedicated radiocarbon AMS systems was taken at ETH Zurich by implementing a vacuum insulated high voltage platform charged to about 200 kV by a conventional solid state power supply. The first radiocarbon dating system of this kind, MICADAS,<sup>[38]</sup> became operational in 2004. With a footprint of only 2.5 m  $\times$  3 m, this is the smallest AMS instrument capable of high-performance radiocarbon measurements. Several improvements of the system were achieved by using He-gas as stripping medium,<sup>[39]</sup> and fixed field magnets incorporating permanent magnetic materials.<sup>[40]</sup> The latter can be regarded as a step towards sustainability because it significantly reduces energy consumption ( $\approx 2$  kW power from the grid in full operation mode). Since 2016 these instruments are commercially available from ETH spinoff company Ionplus AG, and more than 30 MICADAS systems are in operation worldwide. Recently, HVE is also offering a vacuum insulated dedicated radiocarbon AMS system.<sup>[41]</sup> The design principle of this instrument follows to a large extent the ideas on which the MICADAS setup is based.

## 7. Other AMS Nuclides

### 7.1 $^{10}\text{Be}$

The AMS detection method for  $^{10}\text{Be}$  was developed by Raisbeck.<sup>[42]</sup> Most critical is the suppression of the isobaric  $^{10}\text{B}$ . In contrast to beryllium, boron readily forms negative ions. More efficiently,  $\text{BeO}^-$  ions can be extracted from a sputter ion source but the isobaric counterpart  $\text{BO}^-$  is produced as well. To separate the nuclear isobars, their different behavior while passing through matter can be exploited. The nuclear charges of boron and beryllium are 5 and 4, respectively. Thus, the stopping power of boron is much higher, and separation of both ion species can be achieved exploiting their different ranges in matter at a fixed initial ion energy. An absorber mounted in front of a gas ionization chamber can substantially reduce boron ions while beryllium ions can enter the sensitive area of a gas ionization detector. This works very well at MeV energies and unambiguous  $^{10}\text{Be}$  identification can be achieved using foil absorbers in front of a gas ionization detector. AMS systems based on a large accelerator with terminal voltages of 5–8 MV HARVAR foils are used<sup>[43]</sup> and detection limits of  $^{10}\text{Be}/^9\text{Be}$  well below  $10^{-16}$  were reported.<sup>[44]</sup> At lower energies, silicon nitride foils are best suited since their superior homogeneity<sup>[15]</sup> will lead to residual energy distribution as calculated from energy loss straggling only. This provides best conditions for the subsequent separation of  $^{10}\text{Be}$  from  $^{10}\text{B}$  particles in the active volume of the gas ionization counter. At the Vienna Environmental Research Accelerator (VERA) overall efficiency of 45% has been achieved using this method.<sup>[45]</sup>

But it turned out that even at ion energies below 1 MeV a sufficient isobar separation can be achieved. By inserting an energy

degrader foil in front of an energy dispersive beam transport element (e.g. ESA), the two ion species can be spatially separated at the focal plane of this element. By blocking the trajectories of the interfering boron ions with the help of an aperture, the isobaric interference can be reduced. Such a degrader foil (silicon nitrate membranes with thicknesses of a few tenths of nm) is typically inserted after the first magnet at the high energy end of an AMS system. Ions will emerge from such a degrader in different charge states. The following dispersive element will select only ions in one specific charge state and respective beam losses of all other ions must be encountered. The energy spread introduced by the straggling process when heavy ions penetrate matter will cause beam losses, too. This can be compensated for to a large extent, if the energy dispersive action of the ESA is reversed by the opposite energy dispersion of a magnetic dipole spectrometer and achromatic beam transport is achieved from the degrader foil to the final detection system (Fig. 2). A careful optimization of this procedure at compact low energy AMS systems makes overall ion transmission efficiencies (from ion source to the final detection) of more than 10–15% possible.<sup>[46]</sup>

### 7.2 Actinides

At the 3 MV IsoTrace facility<sup>[47]</sup> AMS measurements of actinides were pioneered and the first AMS detection of <sup>236</sup>U was reported using the accelerating voltage of 1.6 MV and detecting the 5<sup>+</sup> ions. AMS laboratories around the world based on large accelerator facilities have dedicated actinide beam lines (ANU,<sup>[48]</sup> Ansto,<sup>[49]</sup> Livermore,<sup>[50]</sup> Vera,<sup>[51]</sup> Cologne<sup>[52]</sup>) and complex measurement arrangements have been installed. In general, a high-resolution electrostatic analyzer with bending radii of up to 2.5 m<sup>[49]</sup> have been incorporated into the high energy beam line, but also Wien-filter systems and additional Time-of-flight detector are in use. An overview on actinide specific measuring technologies can be found in Fifield.<sup>[53]</sup> At ETH Zurich, it has been shown that AMS of plutonium can be performed equally well on a small accelerator operating at only 0.3 MV.<sup>[54]</sup> In fact, this achieved the highest transmission of any AMS system for actinides. Fig. 6 shows a picture of the Multi-Isotope-Low-Energy-AMS system (MILEA) developed in collaboration of ETH Zurich and Ionplus AG.<sup>[55]</sup>

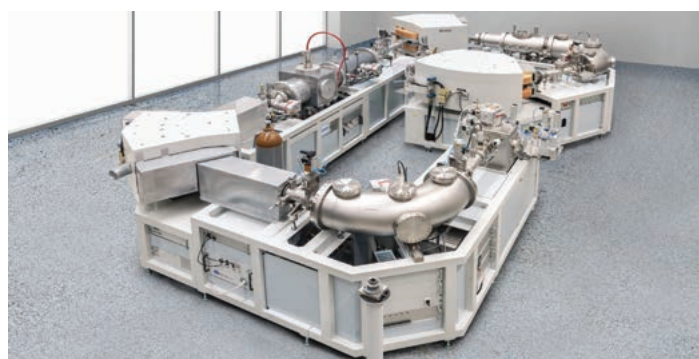


Fig. 6. Multi-isotope low energy AMS system (MILEA) as operated at ETH Zurich.

### 7.3 Nuclides with Isobaric Interference

Separation of nuclear isobars by means of the difference in stopping power is routinely applied for <sup>36</sup>Cl detection. Several AMS facilities based on 5–6 MV tandem accelerators can reach ion energy between 30–50 MeV, which is sufficient to suppress the <sup>36</sup>S isobaric interference while identifying ions in the final particle detector. Typical isobar suppression factors at such energies are 10<sup>4</sup>–10<sup>5</sup> making detection limits beyond the 10<sup>-15</sup> level possible. Gas-filled magnets<sup>[56]</sup> can add additional <sup>36</sup>S suppression capabilities. If the

volume inside the gap of a magnetic dipole spectrometer is filled with gas at low pressure (few hPa), ions passing the magnetic field will undergo frequent collisions changing the actual charge state respectively. They will develop a mean charge state  $\langle q \rangle$  and trajectories will approach a mean bending radius proportional to the  $p/\langle q \rangle$  ratio. Since  $\langle q \rangle$  is depending on ion velocity and nuclear charge, a spatial separation of nuclear isobars results, and by blocking the interfering isobaric beam using an aperture, the intensity of <sup>36</sup>S ion reaching the detector can be reduced significantly. This technology has also been exploited for the detection of radionuclides with  $m > 36$  amu.<sup>[57]</sup> Separations of <sup>53</sup>Mn against <sup>53</sup>Cr, <sup>60</sup>Fe/<sup>60</sup>Ni, and <sup>63</sup>Ni/<sup>63</sup>Cu, <sup>90</sup>Sr/<sup>90</sup>Zr have been achieved at large AMS facilities.<sup>[58]</sup> The high ion energy will help to get isobar discrimination based on the different stopping power of isobars. However, the higher the nuclear charge, the lower the relative energy loss differences and effective isobar suppression becomes practically impossible even at AMS system operating accelerators with 14 MV terminal voltage. A feasible alternative will be Laser and ion cooler techniques which already gain nuclear isobar suppression at the low energy end of an AMS system.<sup>[9,59]</sup> This will be the future to extend the range of AMS nuclides even at small and compact AMS instruments.

### 8. Conclusions

The progress in AMS instrumentation has initiated a growing AMS community. The key feature of AMS to analyze atomic ions in a multi-stage mass spectrometer can be realized by exploiting collisional molecular break-up in an appropriate stripper gas at low ion energies. Dedicated radiocarbon systems have now reached a level of complexity comparable to state-of-the-art mass spectrometers. They are commercially available, do not require personnel as it would be needed in the past to maintain complex accelerator infrastructures, and can provide measurements accuracy at the 1‰ level. But low energy AMS is not limited to radiocarbon detection only. The important AMS nuclides can already be detected at ion energies below 1 MeV. Especially, for the detection of actinide nuclides they benefit from compact designs and high ion transport efficiencies. However, there is not the one and only AMS setup that provides optimum measurement conditions for all AMS nuclides and certain compromises are needed to cover a wide spectrum of nuclides. In general, dedicated systems tailored to the detection to a specific nuclide will outperform systems designed as multi-purpose/multi-nuclide instruments. Medium heavy nuclides with isobaric interferences can still be detected most efficiently at MeV ion energies requiring 6–14 MV accelerator facilities. New developments with isobar suppression exploiting chemical reaction cells and Laser light interaction may quickly evolve into routine operation mode and eventually, unexplored nuclides become accessible with AMS technology.

Received: October 29, 2021

- [1] a) W. F. Libby, E. C. Anderson, J. R. Arnold, *Science* **1949**, *109*, 227; b) J. R. Arnold, W. F. Libby, *Science* **1949**, *110*, 678, <https://doi.org/10.1126/science.110.2869.678>.
- [2] H. Oeschger, J. Houtermans, H. Loosli, M. Wahlen, 12th Nobel Symposium, **1970**, 487.
- [3] K. H. Purser, R. B. Liebert, A. E. Litherland, R. P. Beukens, H. E. Gove, C. L. Bennett, M. R. Clover, W. E. Sondheim, *Rev. Phys. Appl.* **1977**, *12*, 1487, <https://doi.org/10.1051/rphysap:0197700120100148700>.
- [4] Y. Liu, US Patent: 4037100 Appl. no:662968, 1977.
- [5] a) D. E. Nelson, R. G. Korteling, W. R. Stott, *Science* **1977**, *198*, 507, <https://doi.org/10.1126/science.198.4316.507>; b) C. L. Bennett, R. P. Beukens, M. R. Clover, H. E. Gove, R. B. Liebert, A. E. Litherland, K. H. Purser, W. E. Sondheim, *Science* **1977**, *198*, 508, <https://doi.org/10.1126/science.198.4316.508>.
- [6] W. Kutschera, *Int. J. Mass Spectrom.* **2013**, *349–350*, 203, <https://doi.org/10.1016/j.ijms.2013.05.023>.
- [7] Y. Liu, C. C. Havener, T. L. Lewis, A. Galindo-Uribarri, J. R. Beene, AIP Conf. Proc. **2009**, 1099, 737, <https://doi.org/10.1063/1.3120143>.

- [8] A. E. Litherland, *Nucl. Instr. Meth. B* **1994**, *92*, 207, [https://doi.org/10.1016/S0168-583X\(96\)00736-7](https://doi.org/10.1016/S0168-583X(96)00736-7).
- [9] M. Martschini, J. Lachner, K. Hain, M. Kern, O. Marchhart, J. Pitters, A. Priller, P. Steier, A. Wiedering, A. Wieser, R. Golser, *Radiocarbon* **2021**, *1*, <https://doi.org/10.1017/RDC.2021.73>.
- [10] H. J. Hofmann, G. Bonani, M. Suter, W. Wölffi, *Nucl. Instr. Meth. B* **1987**, *29*, 100, [https://doi.org/10.1016/0168-583X\(87\)90214-X](https://doi.org/10.1016/0168-583X(87)90214-X).
- [11] a) M. Suter, S. Jacob, H. A. Synal, *Nucl. Instr. Meth. B* **1997**, *123*, 148, [https://doi.org/10.1016/S0168-583X\(96\)00613-1](https://doi.org/10.1016/S0168-583X(96)00613-1); b) H. A. Synal, S. Jacob, M. Suter, *Nucl. Instr. Meth. B* **2000**, *161*, 29, [https://doi.org/10.1016/S0168-583X\(00\)00359-1](https://doi.org/10.1016/S0168-583X(00)00359-1).
- [12] a) K. H. Purser, R. J. Schneider, J. M. Dobbs, R. Post, Proc. Symp on AMS, **1981**, 431; b) M. Suter, R. Balzer, G. Bonani, W. Wölffi, *Nucl. Instr. Meth. Phys. Res. B* **1984**, *5*, 242, [https://doi.org/10.1016/0168-583X\(84\)90519-6](https://doi.org/10.1016/0168-583X(84)90519-6).
- [13] D. Shapira, R. M. Devries, H. W. Fulbright, J. Töke, M. R. Clover, *Nucl. Instr. Meth.* **1975**, *129*, 123, [https://doi.org/10.1016/0029-554X\(75\)90121-4](https://doi.org/10.1016/0029-554X(75)90121-4).
- [14] a) L. K. Fifield, T. R. Ophel, J. R. Bird, G. E. Calf, G. B. Allison, A. R. Chivas, *Nucl. Instr. Meth. B* **1987**, *29*, 114, [https://doi.org/10.1016/0168-583X\(90\)90412-N](https://doi.org/10.1016/0168-583X(90)90412-N); b) H. A. Synal, J. Beer, G. Bonani, H. J. Hofmann, M. Suter, W. Wölffi, *Nucl. Instr. Meth. B* **1987**, *29*, 146, [https://doi.org/10.1016/0168-583X\(87\)90224-2](https://doi.org/10.1016/0168-583X(87)90224-2).
- [15] M. Döbeli, C. Kottler, M. Stocker, S. Weinmann, H. A. Synal, M. Grajcar, M. Suter, *Nucl. Instr. Meth. B* **2004**, *219-20*, 415, <https://doi.org/10.1016/j.nimb.2004.01.093>.
- [16] A. M. Müller, M. Döbeli, M. Suter, H.-A. Synal, *Nucl. Instr. Meth. Phys. Res. B* **2012**, *287*, 94, <https://doi.org/10.1016/j.nimb.2012.06.012>.
- [17] A. M. Müller, M. Döbeli, H.-A. Synal, *Nucl. Instr. Meth. Phys. Res. B* **2017**, *407, 40*, <https://doi.org/10.1016/j.nimb.2017.05.020>.
- [18] M. G. Klein, D. J. W. Mous, A. Gottgang, *Nucl. Instr. Meth. Phys. Res. B* **2006**, *249*, 764, <https://doi.org/10.1016/j.nimb.2006.03.135>.
- [19] H.-A. Synal, Proc. 11th Int. Conf. on Heavy Ion Accelerator Technology, **2009**, WE.
- [20] S. Maxeiner, M. Suter, M. Christl, H.-A. Synal, *Nucl. Instr. Meth. Phys. Res. B* **2015**, *361*, 237, <https://dx.doi.org/10.1016/j.nimb.2015.04.038>.
- [21] a) H. W. Lee, A. Galindo-Uribarri, K. H. Chang, L. R. Kilius, A. E. Litherland, *Nucl. Instr. Meth. Phys. Res. B* **1984**, *5*, 208, [https://doi.org/10.1016/0168-583X\(84\)90511-1](https://doi.org/10.1016/0168-583X(84)90511-1); b) A. E. Litherland, *Nucl. Instr. Meth. Phys. Res. B* **1984**, *5*, 100, [https://doi.org/10.1016/0168-583X\(84\)90491-9](https://doi.org/10.1016/0168-583X(84)90491-9).
- [22] S. A. W. Jacob, M. Suter, H. A. Synal, *Nucl. Instr. Meth. B* **2000**, *172*, 235, [https://doi.org/10.1016/S0168-583X\(00\)00205-6](https://doi.org/10.1016/S0168-583X(00)00205-6).
- [23] a) M. Suter, R. Huber, S. A. W. Jacob, H.-A. Synal, J. B. Schroeder, AIP Conf. Proc.: 'Application of Accelerators in Research and Industry', Denton, Texas, USA; Eds. J. L. Duggan, I. L. Morgan, **1999**, 665; b) H. A. Synal, S. Jacob, M. Suter, *Nucl. Instr. Meth. Phys. Res. B* **2000**, *172*, 1.
- [24] T. Schulze-König, M. Seiler, M. Suter, L. Wacker, H.-A. Synal, *Nucl. Instr. Meth. B* **2011**, *269*, 34, <https://doi.org/10.1016/j.nimb.2010.09.015>.
- [25] M. Suter, S. Maxeiner, H.-A. Synal, C. Vockenhuber, *Nucl. Instr. Meth. Phys. Res. B* **2018**, *437*, 116 <https://doi.org/10.1016/j.nimb.2018.08.014>.
- [26] P. Sigmund, K. B. Winterbon, *Nucl. Instr. Meth.* **1974**, *119*, 541.
- [27] E. Chamizo, J. M. Lopez-Gutierrez, A. Ruiz-Gomez, F. J. Santos, M. Garcia-Leon, C. Maden, V. Alfimov, *Nucl. Instr. Meth. B* **2008**, *266*, 2217, <https://doi.org/10.1016/j.nimb.2008.02.061>.
- [28] J. Lachner, M. Christl, C. Vockenhuber, H.-A. Synal, *Phys. Rev.* **2012**, *A85*, 022717, <https://doi.org/10.1103/PhysRevA.85.022717>.
- [29] P. G. M. Christl, S. Maxeiner, A. M. Müller, C. Vockenhuber, H.-A. Synal, *Nucl. Instr. Meth. B*, to be published.
- [30] H. A. Synal, M. Stocker, M. Suter, *Nucl. Instr. Meth. B* **2007**, *259*, 7, <https://doi.org/10.1016/j.nimb.2007.01.138>.
- [31] C. Vockenhuber, I. Ahmad, R. Golser, W. Kutschera, V. Liechtenstein, A. Priller, P. Steier, S. Winkler, *Int. J. Mass Spectrom.* **2003**, *223-224*, 713, [https://doi.org/10.1016/S1387-3806\(02\)00944-2](https://doi.org/10.1016/S1387-3806(02)00944-2).
- [32] K. M. Wilcken, M. Hotchkis, V. Levchenko, D. Fink, T. Hausser, R. Kitchen, *Nucl. Instr. Meth. Phys. Res. B* **2015**, *361*, 133, <https://doi.org/10.1016/j.nimb.2015.04.054>.
- [33] K. H. Purser, T. Smick, A. E. Litherland, R. P. Beukens, W. E. Kieser, L. R. Kilius, *Nucl. Instr. Meth. B* **1988**, *35*, 284, [https://doi.org/10.1016/0168-583X\(88\)90284-4](https://doi.org/10.1016/0168-583X(88)90284-4).
- [34] G. A. Jones, A. P. McNichol, K. F. v. Reden, R. J. Schneider, *Nucl. Instr. Meth. Phys. Res. B* **1990**, *52*, 278, [https://doi.org/10.1016/0168-583X\(90\)90421-P](https://doi.org/10.1016/0168-583X(90)90421-P).
- [35] K. F. von Reden, R. J. Schneider, G. J. Cohen, G. A. Jones, *Nucl. Instr. Meth. B* **1994**, *92*, 7.
- [36] M. L. Roberts, R. A. Culp, D. K. Dvoracek, G. W. L. Hodgins, M. P. Neary, J. E. Noakes, *Nucl. Instr. Meth. Phys. Res. B* **2004**, *223-224*, 1, <https://doi.org/10.1016/j.nimb.2004.04.004>.
- [37] J. B. Schroeder, T. M. Hauser, G. M. Klody, G. A. Norton, *Radiocarbon* **2004**, *46*, 1, <https://doi.org/10.1017/S003382220003928X>.
- [38] H. A. Synal, M. Döbeli, S. Jacob, M. Stocker, M. Suter, *Nucl. Instr. Meth. B* **2004**, *223-24*, 339, <https://doi.org/10.1016/j.nimb.2004.04.067>.
- [39] E. Bard, T. Tuna, Y. Fagault, L. Bonvalot, L. Wacker, S. Fahrni, H.-A. Synal, *Nucl. Instr. Meth. Phys. Res. B* **2015**, *361*, 80, <https://doi.org/10.1016/j.nimb.2015.01.075>.
- [40] F. B. Bødker, L. O. Baandrup, N. Hauge, K. F. Laurberg, G. Nielsen, A. Baurichter, B. R. Nielsen, F. B. Bendixen, P. Valler, P. Kjeldsteen, H. D. Thomsen, O. Balling, S. P. Møller, H. A. Synal, in Proc. IPAC2013, Shanghai, China, **2013**, p. 3511.
- [41] M. Klein, N. C. Podaru, D. J. W. Mous, *Radiocarbon* **2019**, *61*, 1441, <https://doi.org/10.1017/RDC.2019.73>.
- [42] G. M. Raisbeck, F. Yiou, D. Bourles, J. Lestrin-guez, D. Deboffe, *Nucl. Instr. Meth. B* **1984**, *5*, 175, [https://doi.org/10.1016/0168-583X\(87\)90196-0](https://doi.org/10.1016/0168-583X(87)90196-0).
- [43] S. Xu, A. B. Dougans, S. P. H. T. Freeman, C. Schnabel, K. M. Wilcken, *Nucl. Instr. Meth. Phys. Res. B* **2010**, *268*, 736, <https://doi.org/10.1016/j.nimb.2009.10.018>.
- [44] D. H. Rood, S. Hall, T. P. Guilderson, R. C. Finkel, T. A. Brown, *Nucl. Instr. Meth. Phys. Res. B* **2010**, *268*, 730, <https://doi.org/10.1016/j.nimb.2009.10.016>.
- [45] P. Steier, M. Martschini, J. Buchriegler, J. Feige, J. Lachner, S. Merchel, L. Michlmayr, A. Priller, G. Rugel, E. Schmidt, A. Wallner, E. M. Wild, R. Golser, *Int. J. Mass Spectrom.* **2019**, *444*, 116175, <https://doi.org/10.1016/j.ijms.2019.116175>.
- [46] A. M. Müller, M. Christl, J. Lachner, M. Suter, H.-A. Synal, *Nucl. Instr. Meth. Phys. Res. B* **2010**, *17-18*, 2801, <https://doi.org/10.1016/j.nimb.2010.05.104>.
- [47] X. L. Zhao, M. J. Nadeau, L. R. Kilius, A. E. Litherland, *Nucl. Instr. Meth. B* **1994**, *92*, 249, [https://doi.org/10.1016/0168-583X\(94\)96014-3](https://doi.org/10.1016/0168-583X(94)96014-3).
- [48] L. K. Fifield, R. G. Cresswell, M. L. di Tada, T. R. Ophel, J. P. Day, A. P. Clacher, S. J. King, N. D. Priest, *Nucl. Instr. Meth. Phys. Res. B* **1996**, *117*, 295, [https://doi.org/10.1016/0168-583X\(96\)00287-X](https://doi.org/10.1016/0168-583X(96)00287-X).
- [49] M. A. C. Hotchkis, D. Child, D. Fink, G. E. Jacobsen, P. J. Lee, N. Mino, A. M. Smith, C. Tuniz, *Nucl. Instr. Meth. Phys. Res. B* **2000**, *172*, 659, [https://doi.org/10.1016/S0168-583X\(00\)00146-4](https://doi.org/10.1016/S0168-583X(00)00146-4).
- [50] T. A. Brown, A. A. Marchetti, R. E. Martinelli, C. C. Cox, J. P. Knezovich, T. F. Hamilton, *Nucl. Instr. Meth. Phys. Res. B* **2004**, *223-224*, 788, <https://doi.org/10.1016/j.nimb.2004.04.146>.
- [51] P. Steier, R. Golser, W. Kutschera, V. Liechtenstein, A. Priller, A. Valenta, C. Vockenhuber, *Nucl. Instr. Meth. Phys. Res. B* **2002**, *188*, 283, [https://doi.org/10.1016/S0168-583X\(01\)01114-4](https://doi.org/10.1016/S0168-583X(01)01114-4).
- [52] A. Dewald, S. Heinze, J. Jolie, A. Zilges, T. Dunai, J. Rethemeyer, M. Melles, M. Staubwasser, B. Kuczewski, J. Richter, U. Radtke, F. von Blanckenburg, M. Klein, *Nucl. Instr. Meth. Phys. Res. B* **2013**, *294*, 18, <https://doi.org/10.1016/j.nimb.2012.04.030>.
- [53] L. K. Fifield, *Quaternary Geochronology* **2008**, *3*, 276, <https://doi.org/10.1016/j.quageo.2007.10.003>.
- [54] L. K. Fifield, H. A. Synal, M. Suter, *Nucl. Instr. Meth. Phys. Res. B* **2004**, *223-224*, 802, <https://doi.org/10.1016/j.nimb.2004.04.148>.
- [55] S. Maxeiner, H.-A. Synal, M. Christl, M. Suter, A. Müller, C. Vockenhuber, *Nucl. Instr. Meth. Phys. Res. B* **2019**, *439*, 84, <https://doi.org/10.1016/j.nimb.2018.11.028>.
- [56] M. Paul, B. G. Glagola, W. Henning, J. G. Keller, W. Kutschera, Z. Liu, K. E. Rehm, B. Schneck, R. H. Siemssen, *Nucl. Instr. Meth. Phys. Res. A* **1989**, *277*, 418, [https://doi.org/10.1016/0168-9002\(89\)90771-7](https://doi.org/10.1016/0168-9002(89)90771-7).
- [57] G. Korschinek, T. Faestermann, S. Kastel, K. Knie, H. J. Maier, J. Fernandezliello, M. Rothenberger, L. Zerle, *Nucl. Instr. Meth. B* **1994**, *92*, 146, [https://doi.org/10.1016/0168-583X\(94\)95995-1](https://doi.org/10.1016/0168-583X(94)95995-1).
- [58] K. Knie, T. Faestermann, G. Korschinek, G. Rugel, W. Rühm, C. Wallner, *Nucl. Instr. Meth. Phys. Res. B* **2000**, *172*, 717, [https://doi.org/10.1016/S0168-583X\(00\)00103-8](https://doi.org/10.1016/S0168-583X(00)00103-8).
- [59] J. Lachner, C. Marek, M. Martschini, A. Priller, P. Steier, R. Golser, *Nucl. Instr. Meth. Phys. Res. B* **2019**, *456*, 163, <https://doi.org/10.1016/j.nimb.2019.05.061>.

#### License and Terms



This is an Open Access article under the terms of the Creative Commons Attribution License CC BY 4.0. The material may not be used for commercial purposes.

The license is subject to the CHIMIA terms and conditions: (<https://chimia.ch/chimia/about>).

The definitive version of this article is the electronic one that can be found at <https://doi.org/10.2533/chimia.2022.45>